Molecular Biology of the Cell
Vol. 21, 2066–2077, June 15, 2010

Promoter DNA Methylation Patterns of Differentiated Cells Are Largely Programmed at the Progenitor Stage

Anita L. Sørensen, Bente Marie Jacobsen, Andrew H. Reiner, Ingrid S. Andersen, and Philippe Collas

Institute of Basic Medical Sciences, Faculty of Medicine, University of Oslo, and Norwegian Center for Stem Cell Research, 0317 Oslo, Norway

Submitted January 7, 2010; Revised March 16, 2010; Accepted April 8, 2010
Monitoring Editor: Carl-Henrik Heldin

Mesenchymal stem cells (MSCs) isolated from various tissues share common phenotypic and functional properties. However, intrinsic molecular evidence supporting these observations has been lacking. Here, we unravel overlapping genome-wide promoter DNA methylation patterns between MSCs from adipose tissue, bone marrow, and skeletal muscle, whereas hematopoietic progenitors are more epigenetically distant from MSCs as a whole. Commonly hypermethylated genes are enriched in signaling, metabolic, and developmental functions, whereas genes hypermethylated only in MSCs are associated with early development functions. We find that most lineage-specification promoters are DNA hypomethylated and harbor a combination of trimethylated H3K4 and H3K27, whereas early developmental genes are DNA hypermethylated with or without H3K27 methylation. Promoter DNA methylation patterns of differentiated cells are largely established at the progenitor stage; yet, differentiation segregates a minor fraction of the commonly hypermethylated promoters, generating greater epigenetic divergence between differentiated cell types than between their undifferentiated counterparts. We also show an effect of promoter CpG content on methylation dynamics upon differentiation and distinct methylation profiles on transcriptionally active and inactive promoters. We infer that methylation state of lineage-specific promoters in MSCs is not a primary determinant of differentiation capacity. Our results support the view of a common origin of mesenchymal progenitors.

INTRODUCTION

Most human tissues contain populations of stem or progenitor cells. Multipotent cells isolated from adipose tissue, bone marrow, or skeletal muscle harbor mesenchymal stem cell (MSC) characteristics in vitro, such as plastic adherence, proliferation capacity, clonogenicity, immunophenotype, and ability to differentiate into several cell types (De Ugarte *et al*., 2003b; Delorme *et al*., 2006; Kern *et al*., 2006; Peault *et al*., 2007; da Silva *et al*., 2008). Adipose stem cells (ASCs) and bone marrow (BM) MSCs express many similar surface markers (De Ugarte *et al*., 2003a; Kern *et al*., 2006; da Silva *et al*., 2008), similar gene expression profiles (Boquest *et al*., 2005; Shahdadfar *et al*., 2005; Pedemonte *et al*., 2007) and adipogenic, osteogenic, and chondrogenic differentiation potential (De Ugarte *et al*., 2003a; Kern *et al*., 2006). Satellite cells isolated from skeletal muscle can differentiate into myocytes, adipocytes, and osteocytes in vitro and their descendants, muscle progenitor cells (MPCs), can undergo multiple divisions before terminal myogenic differentiation (Peault *et al*., 2007). The overall resemblance of these progenitor cells suggests that they are of related ontogeny. Interestingly, cells called pericytes, with surface markers and multilineage differentiation capacity common to MSCs, have independently been shown to reside within the perivascular compartment of fat, bone marrow, muscle, and other tissues (Dellavalle *et al*., 2007; Crisan *et al*., 2008; Zannettino *et al*., 2008). These observations together raise the hypothesis of a common perivascular origin of MSCs (Crisan *et al*., 2008).

A common ontogeny of MSCs would predict that progenitor cells from various tissues exhibit some "intrinsic" similarity; however, there is currently no strong molecular evidence supporting this view. In an attempt to address this issue, we recently showed by bisulfite genomic sequencing that DNA methylation patterns in a handful of lineage-specific promoters in ASCs, BMMSCs, and MPCs were similar (Sørensen *et al*., 2009). Cytosine methylation in CpG dinucleotides constitutes a developmentally regulated epigenetic mark aiming at silencing genes whose expression is no longer required during development (Jaenisch and Bird, 2003). DNA methylation is carried out by DNA methyltransferases and is a reversible process, although mechanisms of active DNA demethylation remain incompletely unraveled (Ooi and Bestor, 2008). Promoter DNA methylation is not always associated with transcriptional repression. This relationship depends on promoter CpG content, with methylated high CpG promoters being usually inactive, whereas methylated low CpG promoters can either be active or inactive (Weber *et al*., 2007). Interestingly, differentiation of mouse embryonic stem (ES) cells into neuronal progenitors

This article was published online ahead of print in *MBoC in Press* (http://www.molbiolcell.org/cgi/doi/10.1091/mbc.E10–01–0018) on April 21, 2010.

Address correspondence to: Philippe Collas (philippe.collas@medisin.uio.no).

Abbreviations used: ASC, adipose stem cell; BMMSC, bone marrow mesenchymal stem cell; ChIP, chromatin immunoprecipitation; ES, embryonic stem; GO, gene ontology; HCP, high CpG promoter; HPC, hematopoietic progenitor cell; ICP, intermediate CpG promoter; KPC, keratinocyte precursor cell; LCP, low CpG promoter; MeDIP, methyl-DNA immunoprecipitation; MPC, mesenchymal progenitor cell; MSC, mesenchymal stem cell; NPC, neuronal progenitor cell; TSS, transcription start site.

and subsequently into neurons has been shown to be accompanied by few DNA methylation changes, most of which occur during the first step of differentiation (Meissner *et al*., 2008; Mohn *et al*., 2008). The promoter methylation states of progenitor cells isolated from primary human tissues and the extent to which these are altered upon lineage-specific differentiation, however, remain uncharacterized.

Here, we surveyed and characterized DNA methylation profiles of all human RefSeq promoters in relation gene expression and differentiation, in adipose tissue-, bone marrow-, and skeletal muscle-derived mesenchymal progenitors, as well as in bone marrow-derived hematopoietic progenitors. Our data lend molecular support to the view of a common origin of mesenchymal precursors. The results also suggest an epigenetic programming of MSC differentiation potential by coenrichment in trimethylated lysine 4 and 27 on histone H3 over an unmethylated DNA background in promoters of lineage-specification genes.

MATERIALS AND METHODS

Cells

ASCs were purified from the stromal vascular fraction of liposuction material from three donors and cultured (Boquest *et al*., 2005) as a pool. BMMSCs were isolated from marrow aspirates from two donors and cultured as described previously (Shahdadfar *et al*., 2005). $CD34^+$ hematopoietic progenitor cells (HPCs) were isolated from bone marrow (Steidl *et al*., 2004). MPCs (CC-2580; Lonza, Allendale, NJ) were cultured in SkGM skeletal muscle medium (Lonza). Human neuronal progenitor cells (NPCs) were as described previously (Donato *et al*., 2007). Transient-amplifying keratinocyte precursor cells (KPCs) were isolated from epidermal sheets obtained from human neonatal foreskin biopsies with >99% purity based on $CD45^-/CD71^{bri}/\alpha6$ $integrin^{bri}$ marker expression, as described previously (Li and Kaur, 2005). KPCs were flash frozen and used in uncultured state. Isolation, culture, and banking of ASCs, BMMSCs, and HPCs were done according to protocols approved by the Regional Committee for Ethics in Medical Research for Southern Norway (approval S-06387a and S-07043a).

Adipogenic and Myogenic Differentiation

ASCs were cultured to confluence in DMEM/F-12 medium containing 10% fetal calf serum and stimulated for 3 wk with 0.5 mM 1-methyl-3 isobutylxanthine, 1 μM dexamethasone, 10 μg/ml insulin, and 200 μM indomethacin (Boquest *et al*., 2005). Cells were stained with Oil Red-O to visualize lipid droplets. For myogenic differentiation, MPCs at 70% confluence were cultured for 6 d in DMEM containing 2% horse serum (Sørensen *et al*., 2009). Nuclei were stained with hematoxylin and eosin.

Bisulfite Sequencing

Genomic DNA was bisulfite-converted using MethylEasy (Human Genetic Signatures, Sydney, Australia) and amplified by polymerase chain reaction (PCR; Supplemental Table S1). PCR products were cloned into bacteria and sequenced as described previously (Noer *et al*., 2006). CpG methylation information is shown for approximately five bacterial clones.

Methyl-DNA Immunoprecipitation (MeDIP) and Microarray Hybridization

MeDIP was performed in duplicate from 4 μg of DNA as described previously (Weber *et al*., 2007), with minor modifications (Sørensen and Collas, 2009). In brief, genomic DNA was treated with 30 μg/ml RNase A for 2 h at 37°C, diluted to 200 μl, and fragmented to ~200–800 base pairs, with enrichment in ~400-base pair fragments, by sonication on ice. Sonicated DNA was ethanol-precipitated using glycogen as a carrier and dissolved in 60 μl of MilliQ H_2O (Millipore, Billerica, MA). Four micrograms of sonicated DNA was diluted in 450 μl of TE buffer (10 mM Tris-HCl, pH 8.0, and 1 mM EDTA), denatured for 10 min in boiling water, and immediately chilled on ice for 10 min. Fifty-one microliters of 10× immunoprecipitation (IP) buffer (1×: 140 mM NaCl, 10 mM Na-phosphate, pH 7.0, and 0.05% Triton X-100) and 10 μl of 5-methylcytosine antibodies (MAb-5MCYT; Diagenode, Liège, Belgium) were added and incubated for 2 h at 4°C on a rotating wheel. Prewashed Dynabeads M-280 sheep anti-mouse immunoglobulin (Ig)G (Invitrogen, Oslo, Norway) in 40 μl of 1× IP buffer was added and incubated for 2 h at 4°C on a rotator. Samples were collected by magnetic separation, washed, and immune complexes were digested with proteinase K for 3 h at 50°C. DNA was extracted with phenol-chloroform isoamylalcohol, ethanol precipitated, and dissolved in 15 μl of H_2O overnight. Input DNA was fragmented and treated as described above except that no immunoprecipitation step was performed. Precipitated and input DNA was amplified using the WGA-2 Whole Genome Amplification kit (Sigma-Aldrich, St. Louis, MO) and cleaned up using the MinElute PCR purification kit (QIAGEN, Hilden, Germany).

For PCR assays, amplified and purified MeDIP and input DNA were diluted to ~25 ng/μl, and 1 μl was amplified by PCR using primers listed in Supplemental Table S1. PCR conditions were 95°C for 3 min and 30 cycles of 95°C for 30 s, 60°C for 30 s, 72°C for 30 s, followed by 7 min at 72°C. PCR products were visualized in a 1% agarose gel stained with ethidium bromide.

For hybridization to microarrays, input and MeDIP DNA fragments were labeled with Cy3 and Cy5, respectively, and hybridized on Roche-Nimblegen human HG18 RefSeq Promoter arrays (C4226-00-01; Nimblegen, Madison, WI). Signal intensity data were centered on zero using NimbleScan (Johnson *et al*., 2008). From scaled $\log_2$ MeDIP/Input ratios, a 750-base pair window was placed around each consecutive probe and a one-sided Kolmogorov–Smirnov (K-S) test was applied to determine whether probes were drawn from a significantly more positive distribution of intensity $\log_2$ ratios than those in the rest of the array. Resulting score for each probe was the *P*-value from the windowed test around that probe. Using NimbleScan, methylated peak data were generated from *P* values by searching for at least 2 probes with a *P*-value cut-off of 0.01 or less. Data were viewed using Nimblegen SignalMap and deposited under NCBI GEO GSE19795.

Correlation of $\log_2$ MeDIP/Input DNA ratios between replicates were computed using values from MaxTen calculations as described previously (O'Geen *et al*., 2006). This algorithm scores each promoter by finding the highest average $\log_2$ ratio among 10 consecutive probes per tiled region. Plotted MaxTen values were the average values from both MeDIP replicates for each cell type. Metagene calculations of average methylation enrichment over the tiled region were performed as described previously (Dahl *et al*., 2009) by using genes with a high probability of enrichment (K-S ≤0.05).

Chromatin Immunoprecipitation (ChIP) and Microarray Hybridization

ChIP was performed essentially as described previously (Dahl and Collas, 2007). In brief, cells were cross-linked with 1% formaldehyde for 8 min, lysis buffer was added to ~120 μl, and samples were incubated for 5 min on ice. Cells were sonicated to produce fragments of ~400 base pairs. After centrifugation, the supernatant was collected, chromatin was diluted to 0.5 A_{260} units, and 100 μl was incubated with 2.4 μg of antibody coupled to magnetic Dynabeads protein A (Invitrogen) for 2 h at 4°C. After washing the ChIP material, 5 μg of RNAse A was added to the ChIP samples, DNA was eluted with 1% SDS and 50 μg/ml proteinase K for 2 h at 68°C, and DNA was dissolved in 10 μl of MilliQ water. ChIP DNA was analyzed by hybridization to the same promoter arrays as those used in MeDIP experiments. Antibodies to H3K9me3 were from Diagenode (pAb-056-050), H3K27me3 was from Millipore (07-449 [note: ex-Upstate catalog no. 05-851]), and H3K4me3 was from Abcam (Cambridge, United Kingdom; Ab8580).

ChIP and input DNA were amplified using the WGA4 kit (Sigma-Aldrich), cleaned up as described above, and eluted in 30 μl of MilliQ water. ChIP and input DNA fragments were labeled with Cy5 and Cy3, respectively, and hybridized to promoter arrays described above. Data were analyzed using NimbleScan (Johnson *et al*., 2008) and are accessible under NCBI GEO GSE17053. Peaks were detected by searching for at least four probes with a signal above a cut-off value using a 500-base pair sliding window. Ratio data were randomized 20 times to evaluate probability of false positives, and each peak was assigned a false discovery rate of 0.1 or less. Metagene assembly was done from genes with identified peaks as described previously (Dahl *et al*., 2009).

Gene Ontology Analysis

Gene ontology (GO) term enrichments within a target gene set were calculated using Bioconductor GOstats (Falcon and Gentleman, 2007). GOstats identifies functional terms for selected genes and provides a significance of enrichment for a term by giving a p value indicating the probability that the identified term is enriched among the target genes relative to what would be expected by chance based on the number of genes in the genome that belong to this term.

Expression Microarrays

RNA was isolated using RNeasy Mini kit (QIAGEN). Biotin-labeled cRNA (1.5 μg) was hybridized onto Illumina Human-6 v2 Expression BeadChips (Illumina, San Diego, CA). Data were analyzed with Bioconductor (www.bioconductor.org). Present/absent calling relied on a classification based on detection p values calculated by Illumina Beadstudio software. Genes with detection p values ≤0.01 were classified as present, those with p values >0.05 were absent, and the rest were marginal. Microarray expression data are accessible in NCBI GEO database under accession GSE17053.

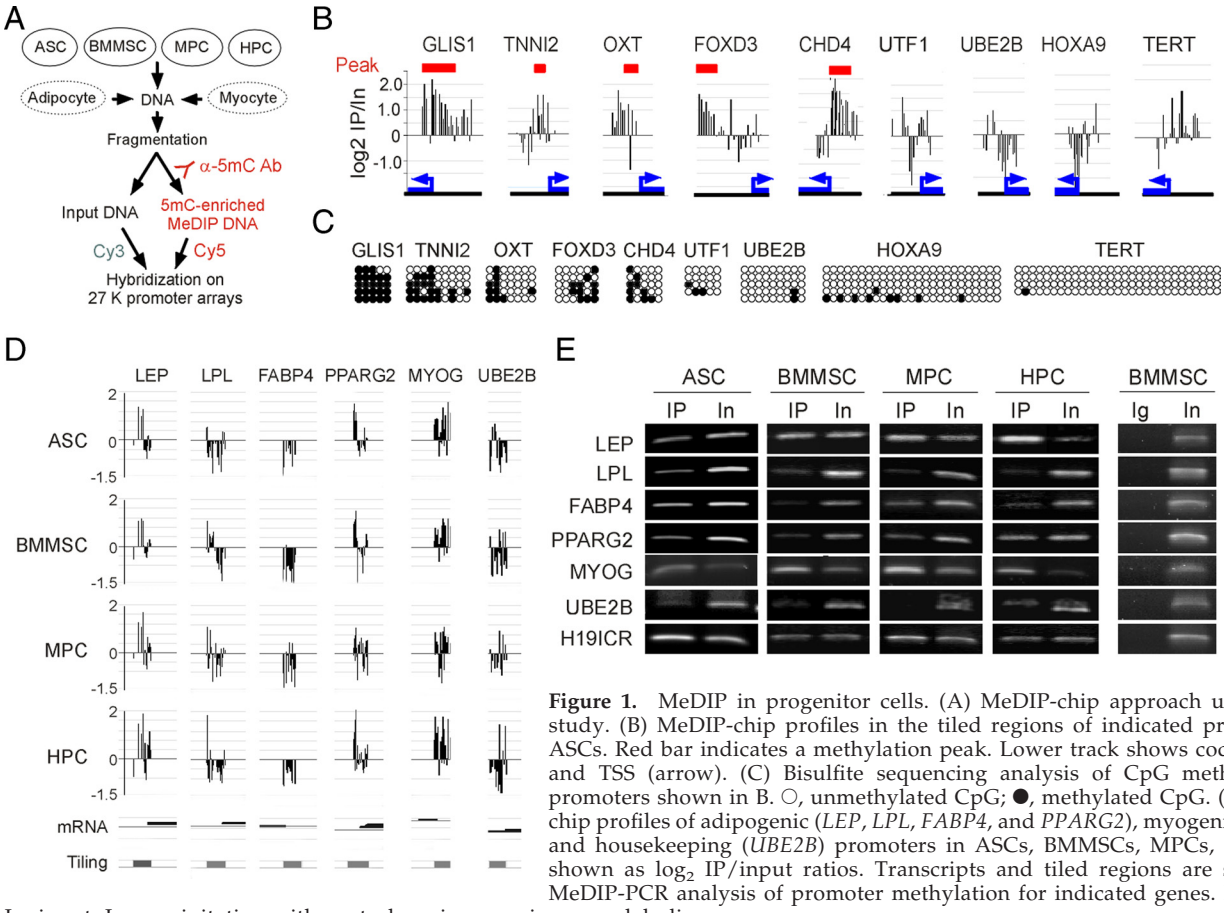

Figure 1. MeDIP in progenitor cells. (A) MeDIP-chip approach used in this study. (B) MeDIP-chip profiles in the tiled regions of indicated promoters in ASCs. Red bar indicates a methylation peak. Lower track shows coding region and TSS (arrow). (C) Bisulfite sequencing analysis of CpG methylation of promoters shown in B. ○, unmethylated CpG; ●, methylated CpG. (D) MeDIP-chip profiles of adipogenic (*LEP*, *LPL*, *FABP4*, and *PPARG2*), myogenic (*MYOG*), and housekeeping (*UBE2B*) promoters in ASCs, BMMSCs, MPCs, and HPCs, shown as $\log_2$ IP/input ratios. Transcripts and tiled regions are shown. (E) MeDIP-PCR analysis of promoter methylation for indicated genes. IP, MeDIP; In, input; Ig, precipitation with control nonimmune immunoglobulin.

RESULTS

Promoter Methylation Profiling of Mesenchymal Progenitor Cells

We addressed the epigenetic relationship, at the DNA methylation level, between progenitor cells isolated from human adipose tissue, bone marrow, and skeletal muscle by MeDIP-chip mapping of promoter DNA methylation profiles in ASCs, BMMSCs, MPCs, and HPCs (Figure 1A). Immunocaptured DNA fragments enriched in 5-methylcytosine were hybridized on promoter arrays tiling −2 kb to +0.5 kb relative to the transcription start site (TSS) of ~27,000 human promoters at 100-base pair resolution. Correlation analysis of $\log_2$ MeDIP/Input ratios for each cell type revealed high reproducibility between replicates (Supplemental Figure S1A).

Validation of the MeDIP approach was done at several levels. MeDIP-chip data were corroborated by bisulfite sequencing of randomly chosen promoters (Figure 1, B and C), by published bisulfite sequencing data for all cell types examined here (Noer *et al.*, 2006; Sørensen *et al.*, 2009) and by MeDIP-PCR single-gene analysis (Figure 1, D and E). MeDIP-PCR data were in addition verified for additional ASC, BMMSC, and MPC donors (Supplemental Figure S2). MeDIP-chip further corroborated published MeDIP-PCR data for methylated and unmethylated promoters in human fibroblasts (Weber *et al.*, 2007) (Supplemental Figure S1, B and C). MeDIP-PCR also confirmed hypomethylation of the housekeeping *UBE2B* promoter and methylation of the *H19* imprinting control region (*H19ICR*) reported previously in fibroblasts (Weber *et al.*, 2007) (Figure 1E). Lastly, the proportions of methylated genes detected by MeDIP-chip in ASCs and BMMSCs (19% of 17,790 RefSeq genes in both cell types) were similar to those detected earlier by combined bisulfite restriction analysis (17 and 16%, respectively) among ~170 genes (Dahl *et al.*, 2008), and methylation patterns reported for those genes, validated by bisulfite sequencing (Dahl *et al.*, 2008), were corroborated by MeDIP-chip data.

Adipose Tissue, Bone Marrow, and Muscle Progenitors Share a Large Set of Hypermethylated Genes

We identified with high significance (K-S test p value ≤0.01 for detection of methylation "peaks") >3300 promoters hypermethylated relative to genome-average methylation in ASCs and BMMSCs, 2630 in MPCs, and 3902 in HPCs (Figure 2A). These made up 15–22% of all RefSeq promoters represented on the array (Figure 2A). Hybridization patterns (Figure 2B) and calculated MaxTen values of methylation intensity for all promoters (Figure 2C) revealed high similarity and overlap between ASCs, BMMSCs, and MPCs. Intersect analysis of promoters with at least one hypermethylation peak showed that ASCs and BMMSCs shared 2486 hypermethylated genes (74% of all hypermethylated genes in these cell types; Figure 2, C and D). ASCs and BMMSCs, respectively, shared 1944 (57%) and 2053 (61%) hypermethylated genes with MPCs (Figure 2, C and D). We also identified a core of 1755 hypermethylated genes common to ASCs, BMMSCs, and MPCs, representing 52–66% of all hypermethylated genes in these cell types (Figure 2D). Another 20–30% was methylated in two of three cell types, whereas 15–20% was methylated only in one cell type (Fig-

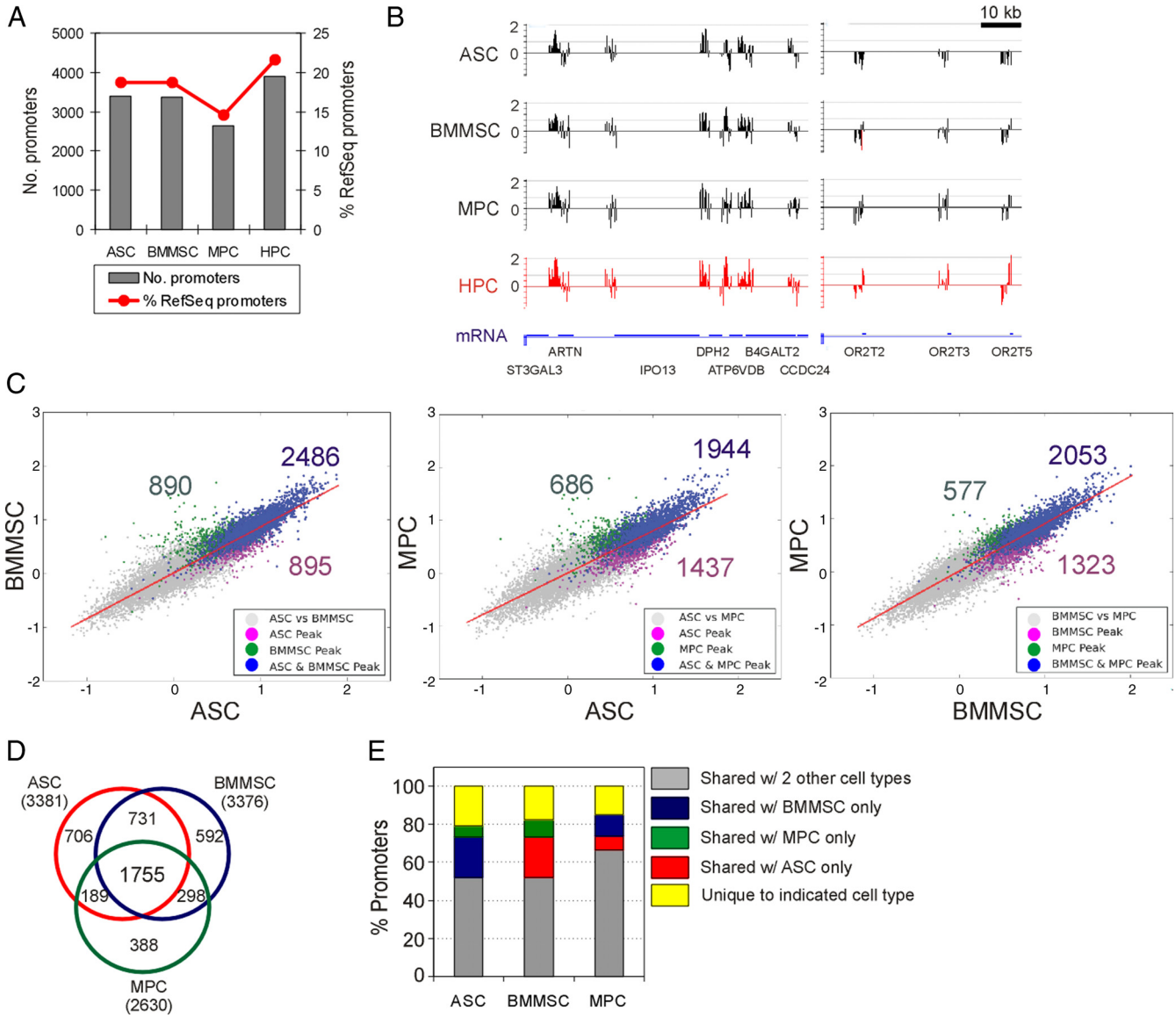

Figure 2. MeDIP-chip analysis of promoter DNA hypermethylation in mesenchymal progenitors. (A) Number and percentage of hypermethylated RefSeq promoters in ASCs, BMMSCs, MPCs, and HPCs. (B) Methylation profiles showing methylated (left) and unmethylated (right) promoters on two segments of chromosome 1 ($\log_2$ IP/input). (C) Two-dimensional scatter plots of MaxTen values of methylation intensity in one cell type versus another. Average MaxTen values of both MeDIP replicates are plotted. Data points were colored to indicate classification according to peak calling algorithm to show hypermethylated promoters in one (purple, green) or both (blue) cell types. (D) Venn diagram analysis of hypermethylated promoters in ASCs, BMMSCs, and MPCs. (E) Percentages of hypermethylated promoters unique to each cell type and shared between cell types, identified from D.

ure 2E). These data indicate a high similarity of promoter DNA methylation patterns in progenitor cells from adipose tissue, bone marrow and skeletal muscle.

To determine whether the hypermethylated gene core was specific to mesenchymal progenitors, we also examined BM-derived CD34$^+$ HPCs. We found that 91% of the 1755 core hypermethylated genes also were hypermethylated in HPCs, whereas HPCs contained 2302 hypermethylated genes that distinguished them from mesenchymal progenitors considered as a whole (Figure 3A). Moreover, 30–50% of genes found to be hypermethylated in ASCs, BMMSCs, or MPCs only (Figure 2D, crescents) were also hypermethylated in HPCs (Supplemental Figure S3). Lists of these genes hypermethylated in ASCs, BMMSCs, and MPCs are provided in Supplemental Table S2.

These results collectively indicate that promoter methylation profiles are similar but not identical among ASCs, BMMSCs, and MPCs, highlighting an intrinsic epigenetic identity between these mesenchymal progenitors. The majority of these genes are also hypermethylated in HPCs, which also contain an additional large set of hypermethylated genes.

Early Developmentally Regulated Genes Are Hypermethylated in Mesenchymal and Nonmesenchymal Progenitors

To address the biological significance of the hypermethylated genes revealed by MeDIP-chip, we identified GO terms enriched among these genes (Figure 3B and Supplemental

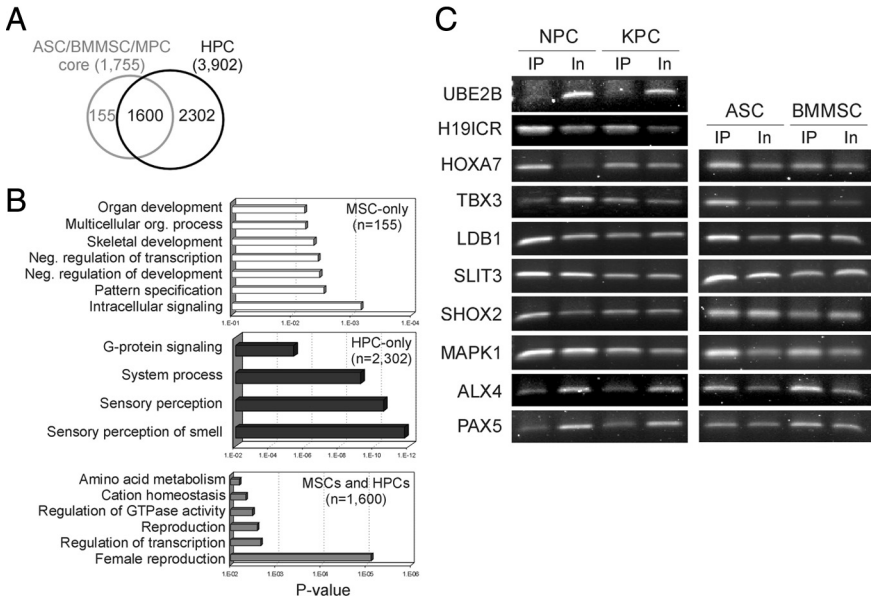

Figure 3. GO term enrichment for genes hypermethylated in MSCs and HPCs. (A) Venn diagram analysis of hypermethylated genes included in the MSC methylation core versus HPCs. (B) Enriched GO terms for genes hypermethylated in MSCs and HPCs. (C) A subset of developmentally regulated promoters is hypermethylated in NPCs and KPCs. MeDIP-PCR analysis of promoter methylation for indicated genes. IP, MeDIP; In, input. *UBE2B* and *H19*ICR methylation states in ASCs and BMMSCs are shown in Figure 1E.

Table S3). Interestingly, genes hypermethylated in MSCs as a whole were enriched in signaling and developmental functions pertaining to early fetal development. Genes hypermethylated in HPCs were enriched in signaling functions linked to sensory perception, whereas genes hypermethylated in both MSCs and HPCs were associated with reproduction processes in addition to signaling, transcription regulation, and metabolic functions (Figure 3B). This finding corroborated the differential epigenetic programming of the germline and the soma shown previously by MeDIP-chip using similar promoter arrays (Weber *et al*., 2007). GO analysis therefore suggests that hypermethylation targets developmental functions disabled at the progenitor stage examined here, as well as late differentiation-associated functions.

A randomly chosen subset of early developmental genes identified above was shown to also be hypermethylated in NPCs and KPCs (Figure 3C), indicating that hypermethylation of these genes can occur in precursors of both mesodermal and ectodermal origin. Nonetheless, among the genes examined some (*TBX3*, *ALX4*, and *PAX5*) were hypomethylated in NPCs and/or KPCs (yet were as expected from our MeDIP-chip data hypermethylated in ASCs and BMMSCs) (Figure 3C), a pattern that may be linked to their role in neurogenesis and keratinocyte function (Asbreuk *et al*., 2002; Norhany *et al*., 2006; Pillai *et al*., 2007).

Differentiation Partly Resolves Promoter Methylation Patterns Common to Mesenchymal Progenitors

MeDIP-chip and bisulfite sequencing data have shown that in vitro differentiation of mouse ES cells into neuronal progenitors and subsequently into neurons is accompanied by remarkably few methylation changes, most of which occur during the first step of differentiation (Meissner *et al*., 2008; Mohn *et al*., 2008). This predicts that at least in this in vitro model, methylation patterns of differentiated cells would be established at the progenitor stage. To address this issue in primary progenitors, ASCs were differentiated in vitro into adipocytes and MPCs were differentiated into multinucleated myocytes. Differentiation was assessed by formation of Oil Red-O–positive lipid inclusions in adipocytes (Figure 4A), formation of multinucleated myocytes (Figure 4A), and up-regulation of lineage-specific genes in microarray expression analyses (Supplemental Table S4).

Promoter methylation changes after differentiation distinguished adipocytes from ASCs and myocytes from MPCs (Figure 4B). Nonetheless, most (~80%) hypermethylated promoters in undifferentiated cells remained hypermethylated (Figure 4C), suggesting that methylation states in differentiated cells are largely established at the progenitor stage. In addition, 29% of all methylated promoters identified in adipocytes were hypermethylated after ASC differentiation, whereas 15% of the methylated promoters in ASCs were hypomethylated (Figure 4, C and D). Similar observations were made after MPC differentiation (Figure 4, C and D). Thus, ASC and MPC differentiation is accompanied by methylation changes leading to an increase in the number of hypermethylated promoters in differentiated cells ($p < 10^{-4}$; chi-square test with Yates' correction).

These data are consistent with enhanced transcriptional restrictions by DNA methylation as cells differentiate. To address the lineage specificity of these methylation changes, we cross-examined genes methylated in adipocytes and myocytes. Twenty percent of genes hypermethylated after differentiation were common to both cell types (Figure 4E). A subset of these genes was involved in stimulation-dependent changes in metabolism, consistent with differentiation induction (Supplemental Figure S4). Eighty percent of the hypermethylated genes, however, were cell type specific (Figure 4E). GO term enrichment analysis indicates that these were involved in the regulation of nuclear assembly, nuclear-cytoplasmic transport, and G-protein signaling in adipocytes (consistent with the completion of nuclear reorganization taking place during the formation of mature adipocytes), and in cell–cell interaction and exocytotic and sensory perception functions in myocytes (Supplemental Figure S4 and Supplemental Table S5). The reduced overlap of hypermethylated genes between adipocytes and myocytes, compared with ASCs and MPCs, reflects a greater epigenetic divergence between the two differentiated cell types than between their respective undifferentiated counterparts.

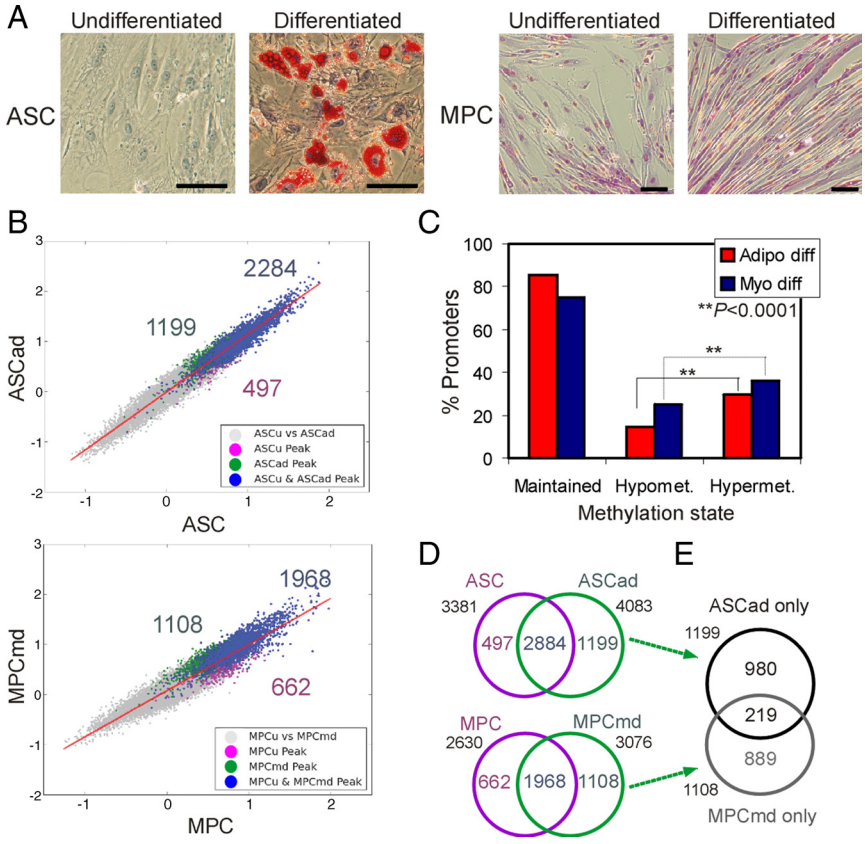

Figure 4. MSC differentiation partially resolves promoter methylation profiles. (A) In vitro differentiation of ASCs into adipocytes (stained with Oil Red-O) and of MPCs into multinucleated myocytes (stained with Hemacolor). Bars, 100 μm. (B) Two-dimensional scatter plots of MaxTen values for methylation intensities in ASCs or MPCs versus their differentiated counterparts (ASCad and MPCmd). Average values of both MeDIP replicates are plotted. Data points were colored to indicate classification according to peak calling to show hypermethylated promoters in differentiated cells (green), undifferentiated cells (purple), and common to both (blue). ASCad, adipogenic-differentiated ASCs; MPCmd, myogenic-differentiated MPCs. (C) Percentage of hypo- and hypermethylated promoters after adipogenic and myogenic differentiation of ASCs and MPCs. Venn diagrams of hypermethylated promoters in undifferentiated versus differentiated ASCs and MPCs (D) and between differentiated ASCs and MPCs (E).

Relationship between Promoter Methylation and Gene Expression upon Differentiation

We next determined the extent to which differentiation-induced changes in promoter methylation reflected transcriptional changes. We first assessed the proportion of expressed genes in ASCs, BMMSCs, and MPCs by using Illumina expression arrays by defining present (expressed), marginal (weakly expressed), and absent (not expressed) cells. In each cell type, 54–57% of the hypermethylated genes were detected as expressed or weakly expressed. These percentages were similar to the proportion of expressed RefSeq genes detected in these cell types irrespective of methylation state (Supplemental Figure S5). Thus, promoter methylation is compatible with transcriptional activity (also see Weber *et al*., 2007).

We next determined transcriptional states associated with promoter hypo- or hypermethylation resulting from differentiation. After adipogenic differentiation, we found 702 genes overexpressed or induced (Supplemental Table S4), 645 of which were included on the Nimblegen platform. Of these, 102 (16%) were hypermethylated in undifferentiated ASCs. Among those methylated genes, 15 became demethylated, whereas 87 retained their methylation state. After myogenic differentiation of MPCs, 444 genes were overexpressed or induced (Supplemental Table S4), 417 of which were covered on the Nimblegen platform. Among those, 49 (12%) were hypermethylated in undifferentiated MPCs. Among those methylated genes, 13 became demethylated, whereas 36 retained their methylation state. These results indicate that the majority of genes up-regulated after MSC differentiation are DNA hypomethylated in undifferentiated cells. Moreover, among hypermethylated genes, only a quarter or less undergo methylation change.

Promoter Methylation Enrichment Profiles Distinguish Promoters of Expressed versus Nonexpressed Genes

We next addressed whether methylation occurred in distinct regions relative to the TSS in expressed versus nonexpressed genes in ASCs, BMMSCs, and MPCs. To this end, we determined average methylation by computing metagene profiles for all hypermethylated promoters. These profiles were distinct for transcriptionally active and inactive promoters (Figure 5A and Supplemental Figure S6). In all cell types, the amplitude of methylation enrichment was greater on promoters of expressed genes than nonexpressed genes (p values from Welsh two-sample t tests for methylation intensity amplitude in ASCs: $p < 2.2 \times 10^{-16}$; BMMSCs: $p = 1.34 \times 10^{-14}$; and MPCs: $p = 3.04 \times 10^{-3}$): enrichment was stronger on active promoters but sharply decreased to genome-average or below immediately 5′ of the TSS. In contrast, on inactive promoters, maximum enrichment was lower but was more widely spread by an additional 500-1500 base pairs to include the TSS, as determined by extension of the width at half-maximal enrichment (Figure 5, A and B, and Supplemental Figure S6). These data indicate that the profile of methylation coverage distinguishes promoters of expressed and nonexpressed genes. Nevertheless, the density of methylated CpGs was lower at the TSS than upstream in both expressed and repressed genes, corroborating recent genome-scale bisulfite sequencing data (Lister *et al*., 2009).

Methylation Preferentially Targets Intermediate and Low CpG Content Promoters

The relationship between promoter DNA methylation and gene activity has been shown to depend on CpG content (Weber *et al*., 2007). Thus, we asked whether methylation

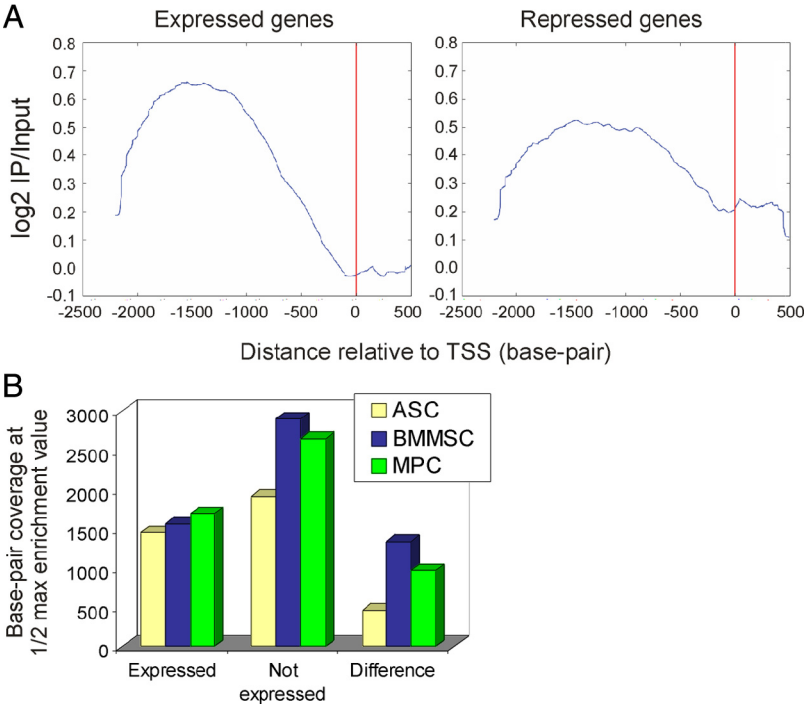

Figure 5. Distinct DNA methylation enrichment profiles on promoters of expressed versus nonexpressed genes. (A) Metagene analysis of average DNA methylation enrichment on hypermethylated promoters of expressed and repressed genes in ASCs. (B) Base pair coverage of methylation on promoters of expressed and nonexpressed genes, shown as width at half-maximal enrichment intensity calculated from metagene profiles. The difference in width at half-maximal enrichment intensity between expressed and nonexpressed genes for each cell type is also shown (right 3 columns).

enrichment detected in the tiled regions in progenitor cells was influenced by promoter CpG content. Previous classification of human RefSeq promoters based on CpG density revealed a bimodal distribution from observed/expected CpG ratios, identifying high (HCP), intermediate (ICP), and low (LCP) CpG promoters (Weber *et al*., 2007). We applied the algorithm of Weber *et al*. (2007) to the tiled regions (−2.5 to +0.5 kb relative to the TSS) of all RefSeq promoters represented on the array, and we identified 11511 HCPs, 3173 ICPs, and 3246 LCPs; these numbers were comparable with those of Weber *et al*. (2007).

In all cell types examined, CpG methylation targeted a higher proportion of ICPs relative to the proportion of ICPs in the genome (Figure 6A; $p < 10^{-4}$; chi-square test with Yates' correction), at the expense of HCPs whose proportion was reduced among methylated promoters ($p < 10^{-3}$ to 10^{-4}). Methylation did not preferentially target LCPs except in hematopoietic progenitors where methylated LCPs were enriched ($p = 0.0005$). Thus, CpG methylation targets a higher proportion of intermediate to low CpG promoters compared with their proportions in the genome, in consistency with the enhanced protection of CpG islands against methylation (Weber *et al*., 2007; Irizarry *et al*., 2009; Straussman *et al*., 2009).

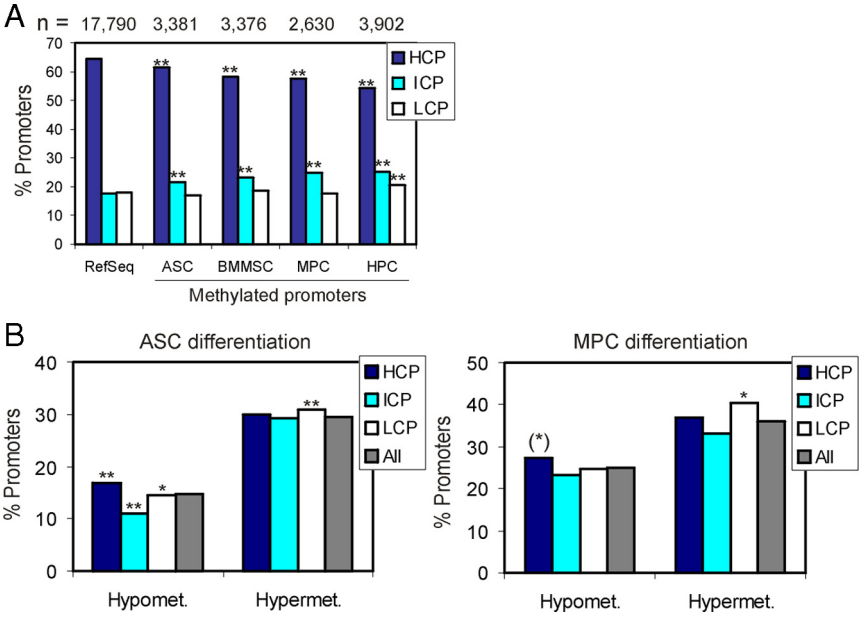

Figure 6. Promoter CpG content differentially affects methylation targeting and methylation response to differentiation induction. (A) Proportion of LCPs, ICPs, and HCPs among hypermethylated genes in ASCs, BMMSCs, MPCs, HCPs, and among all human RefSeq genes. Numbers of genes included in the analysis are shown on top. **$p \leq 0.0005$ relative to the RefSeq data set. (B) Evolution of promoter methylation after adipogenic (left) and myogenic (right) differentiation as a function of promoter CpG class. "All" refers to all hypo- or hypermethylated promoters identified in Figure 4D. **$p \leq 0.0003$, *$p = 0.033$, and (*)$p = 0.077$, relative to the All data set.

Differentiation-induced Methylation Changes Distinctively Affect High- and Low-CpG Content Promoters

Having established that methylation differentially affects promoters with distinct CpG contents, we determined whether the nature of methylation changes (hypo- or hypermethylation) after adipogenic or myogenic differentiation differed between promoter classes. To this end, methylation changes identified in Figure 4D were reanalyzed for HCPs, ICPs, and LCPs. Figure 6B shows that in ASCs, hypomethylated genes were enriched in HCPs ($p = 0.0003$; Fisher's exact test) relative to the total number of hypomethylated genes, at the expense of ICPs ($p < 10^{-4}$) and LCPs ($p = 0.033$). Furthermore, there was an enrichment of hypermethylated genes in LCPs ($p = 0.0004$), whereas HCPs and ICPs were not affected ($p > 0.5$). In MPCs, we also detected a trend in enrichment of hypomethylated genes in HCPs ($p = 0.077$) and an enrichment of hypermethylated genes in LCPs ($p = 0.05$) without significantly affecting HCPs and ICPs (Figure 6B). We concluded that differentiation-elicited hypomethylation predominantly affected methylated HCPs, whereas hypermethylation preferentially concerned LCPs.

Methylation State of Lineage-specific Promoters Is Not a Determinant of Differentiation Capacity

Our previous bisulfite sequencing results suggested no predictability of MSC differentiation capacity based on the methylation state of a few lineage-specific promoters (Sørensen *et al*., 2009). Using our MeDIP-chip data, we extended our analysis of ASCs, BMMSCs, MPCs, and HPCs to 200 lineage-priming genes (including 50 HCPs and 150 non-HCPs) linked to differentiation into mesodermal, endodermal, and ectodermal lineages (Supplemental Table S6). These included 107 lineage-priming genes recently reported to be expressed at least at some level in BMMSCs (Delorme *et al*., 2009). We detected 57 hypermethylated promoters (28.5%) in at least one cell type, of which 8 (4%) were hypermethylated in all cell types. Methylation of these promoters did not occur in any particular developmental lineage for a given cell type, and we did not observe any significant difference in the proportion of hypermethylated promoters between cells, including HPCs. In fact, most promoters specifying mesodermal (adipogenic, osteogenic, chondrogenic, myogenic, and vascular), endodermal (pancreatic, hepatic) and ectodermal (neurogenic, skin) differentiation were not hypermethylated (Supplemental Figure S7 and Supplemental Table S6). These findings confirm the absence of relationship between methylation state and differentiation capacity of MSCs.

DNA-methylated Promoters in ASCs Are in Majority Not Trimethylated on H3K4, H3K9, or H3K27

The lack of straightforward relationship between promoter DNA methylation and MSC differentiation capacity prompted the interrogation of additional epigenetic states on promoters. We examined by ChIP-on-chip in ASCs and in relation to DNA methylation the promoter enrichment profiles for trimethylated lysine 4 of histone H3 (H3K4me3), a transcriptionally permissive modification; H3K27me3, a Polycomb-mediated transcriptionally repressive mark; and H3K9me3, a mark of heterochromatin associated with repressed promoters (Kouzarides, 2007).

We identified 3362 promoters enriched in H3K4me3 and 2321 enriched in H3K27me3 (Figure 7A). GO term enrichment analysis showed that H3K4me3-marked genes were associated with transcription regulation, macromolecule synthesis, and metabolic processes, whereas H3K27me3-marked genes were distinctively enriched in developmental, differentiation and signaling functions (Figure 7B and Supplemental Table S7). Moreover, 25% of H3K4me3 promoters were coenriched in H3K27me3 (Figure 7, A and C) and displayed largely overlapping average enrichment profiles for these modifications, in contrast to promoters exclusively harboring either mark (Figure 7D). Although we do not have formal proof that these modifications co-occupy individual promoters, the metagene profiles together with previous sequential ChIP results (Noer *et al*., 2009) suggest that they might. GO terms enriched among H3K4/K27me3-enriched genes pertained to transcription regulation, development, differentiation, and cell adhesion (Figure 7B and Supplemental Table S7). These functional groups were similar to those of H3K4/K27me3 "bivalent" genes in ESCs (Bernstein *et al*., 2006; Pan *et al*., 2007; Zhao *et al*., 2007), in hematopoietic progenitors (Cui *et al*., 2009) and in embryos (Dahl *et al*., 2010). These findings extend the concept that H3K4/K27me3 coenrichment marks developmentally important promoters in stem and progenitor cells.

We next examined histone modifications associated with DNA methylated promoters (exemplified in Figure 7E). We found that of DNA methylated promoters, 22% were enriched in H3K4me3, 17% were enriched in H3K27me3, and <7% were trimethylated on H3K9 (Figure 7, A and C). These proportions were notably lower than those of H3K4me3-, H3K27me3-, and H3K9me3-enriched promoters among all modified RefSeq promoters (respectively, 37%, 24 and 17%; data not shown; $p < 0.001$; chi-square test with Yates' correction). Thus, DNA methylation and H3K4, K9, or K27 trimethylation seem to be largely exclusive at least in the promoter regions examined. H3K4/K27me3 coenrichment occurs mainly on weakly or unmethylated promoters (Figure 7C), a configuration reminiscent of the DNA hypomethylated state of developmentally regulated bivalent promoters in ES cells (Fouse *et al*., 2008; Mohn *et al*., 2008).

Nonetheless, a nonnegligible proportion of DNA methylated promoters was found to be enriched in H3K4me3 or H3K27me3 (Figure 7, A and C). These genes were enriched linked to transcription regulation, metabolic and synthetic processes (H3K4me3), early development, and differentiation (H3K27me3), or transcription and differentiation (H3K4/K27me3). These functional categories were similar to those defined by H3K4 or H3K27 methylation alone (Supplemental Table S7) and were not altered by DNA methylation states. Moreover, we found that the majority (80 to >90%) of H3K27me3- or H3K9me3-enriched genes were not expressed, whereas 60% of H3K4me3 genes were expressed (data not shown). These percentages were similar among DNA methylated genes and among all RefSeq genes bearing these marks (data not shown); thus, DNA methylation does not confer additional repressive effect on promoters harboring any of these histone modifications.

Trimethylated H3K4 and H4K27 Delineate Distinct Epigenetic Markings on a Subset of DNA-methylated Transcriptionally Active and Inactive Promoters

Our earlier data outlined distinct average DNA methylation enrichment profiles on the promoters of expressed versus nonexpressed genes (Figure 5A). To start addressing the biological significance of this observation, we examined histone modifications patterns on these promoters (Supplemental Figure S8). We first noted that only 23 and 28% of DNA methylated expressed and nonexpressed promoters, respectively, were enriched above genome-average level in any of the histone marks examined (see above). Second, of

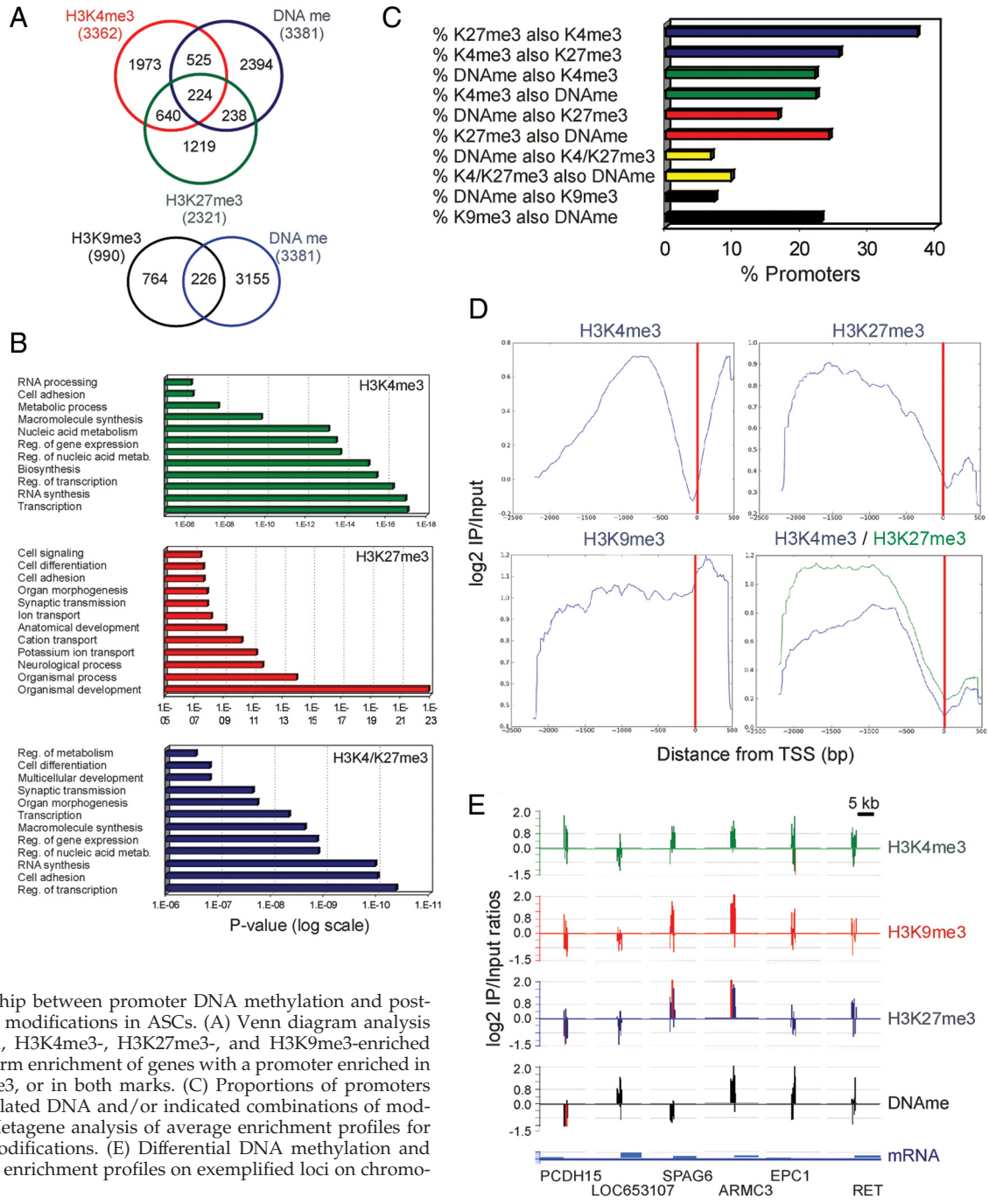

Figure 7. Relationship between promoter DNA methylation and post-translational histone modifications in ASCs. (A) Venn diagram analysis of DNA methylated, H3K4me3-, H3K27me3-, and H3K9me3-enriched promoters. (B) GO term enrichment of genes with a promoter enriched in H3K4me3, H3K27me3, or in both marks. (C) Proportions of promoters coenriched in methylated DNA and/or indicated combinations of modified histones. (D) Metagene analysis of average enrichment profiles for indicated histone modifications. (E) Differential DNA methylation and histone modification enrichment profiles on exemplified loci on chromosome 10.

the active DNA-methylated promoters coenriched in trimethylated H3K4, K9, or K27, 85% were enriched in H3K4me3 alone (74%) or together with H3K27me3 (11%) (Figure 8A, left). A minority harbored H3K9me3 (2%) or H3K27me3 (13%) only, as expected. Inactive DNA-methylated promoters, in contrast, were predominantly enriched in H3K27me3 only (43%) or together with H3K4me3 (25%), or in H3K4me3 only (25%) (Figure 8A, right). H3K9me3 enrichment accounted again for only a minor proportion of these DNA-methylated repressed promoters (7%) at least within the tiled region (Figure 8A, right).

We next determined whether these proportions were different from those among all expressed or repressed RefSeq promoters that are also modified. Figure 8B shows that histone modification enrichment patterns on these promoters were very similar to those of DNA-methylated expressed or repressed promoters. Thus, differential histone modification marking of the promoter of expressed or repressed genes is independent of their DNA methylation state in the genomic regions examined. Lastly, we showed, however, that these histone modification patterns were clearly distinct form those of all RefSeq promoters, regardless of transcriptional status (Figure 8C). Therefore, in addition to the profile of DNA methylation, epigenetic markings such as trimethylated H3K4 and K27, and to a lesser extent K9, delineate distinct chromatin states on a subset of transcriptionally

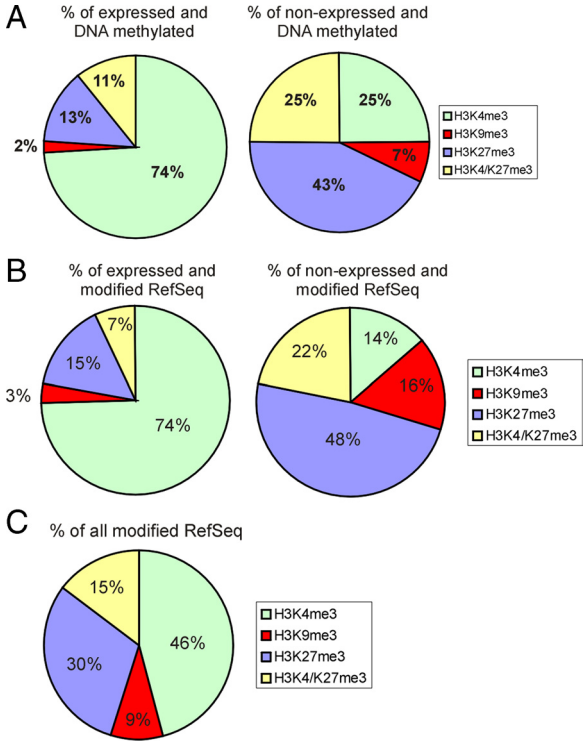

Figure 8. Promoters of expressed and nonexpressed genes are enriched in distinct proportions of trimethylated H3K4, K9, and K27 irrespective of DNA methylation. (A) Histone modifications associated with DNA-methylated promoters of expressed or repressed genes. Percentages were calculated from MeDIP-chip and ChIP-on-chip data, and are those of DNA-methylated promoters also enriched in the indicated histone modifications (see Supplemental Figure S8 for Venn diagrams). (B) Histone modifications associated with all expressed and nonexpressed RefSeq promoters, regardless of DNA methylation. (C) Histone modifications associated with all RefSeq promoters enriched in H3K4me3, H3K9me3, H3K27me3, or in H3K4/K27me3.

active versus inactive promoters (Figure 9A). Of these modifications, however, only H3K9me3 seems to be differentially enriched on DNA hypermethylated versus hypomethylated repressed promoters ($p < 0.01$; chi-square test; Figure 8, A and B).

DISCUSSION

A compilation of phenotypic, transcriptomic, and functional evidence argues that MSCs isolated from various adult tissues may be similar, although not identical (De Ugarte *et al.*, 2003b; Delorme *et al.*, 2006; Kern *et al.*, 2006). The finding that pericytes contain cells with MSC properties has raised the hypothesis that MSCs originate from a common perivascular niche within their respective tissues (Crisan *et al.*, 2008; da Silva *et al.*, 2008; Zannettino *et al.*, 2008). In an analysis of all annotated RefSeq promoters, we show here a similarity of DNA methylation patterns in mesenchymal progenitors from adipose tissue, bone marrow, and skeletal muscle. We propose that a core of hypermethylated genes constitutes a common intrinsic epigenetic marking of ASCs, BMMSCs, and MPCs, lending support to the functional resemblance of MSCs identified in various tissues and to the view of a common origin of MSCs.

Not all pericytes, however, are MSC ascendants because pericytes also include hematopoietic precursors (Kiel and Morrison, 2006). This implies that differentially programmed progenitors coexist with MSCs in specific compartments. We find that 90% of the hypermethylated genes common to MSCs are also hypermethylated in HPCs. These genes are associated with regulation of development, transcription, signaling, and metabolic functions, arguing that promoter methylation contributes to repressing a common array of a wide range of functions in these precursor cells. HPCs also harbor another 2300 hypermethylated genes not identified in MSCs, suggesting that they are more epigenetically distant from MSCs than MSC types are from one another. The endoderm, mesoderm, and ectoderm specification and differentiation functions of genes hypermethylated in HPCs are consistent with an additional developmental restriction of HPCs relative to MSCs.

Does promoter methylation in progenitor cells reflect lineage programming, or pathways and processes no longer enabled at this stage of differentiation? We have recently proposed that strong methylation of lineage-specification promoters may impose a restriction on differentiation capacity (e.g., adipogenic and myogenic potential in HPCs, or

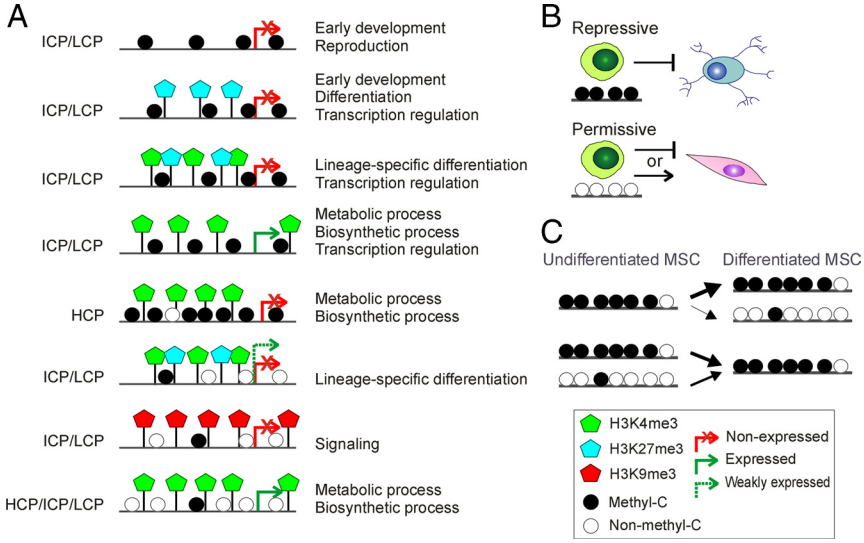

Figure 9. Chromatin states in human mesenchymal stem cells. (A) DNA methylation and histone modification patterns are grouped into several combinations on promoters of genes involved in indicated cellular functions. Promoter CpG content is shown on the left. (B) Model of MSC differentiation capacity in relation to DNA methylation of lineage-specific promoters. Hypermethylation is likely to be repressive; hypo- or unmethylation constitutes a permissive configuration, although it is of no predictive value on differentiation potential. (C) Changes in promoter DNA methylation after MSC differentiation: summary drawn from adipogenic ASC differentiation and myogenic MPC differentiation. Thickness of arrows reflects the proportion of promoters undergoing the indicated methylation change, or absence thereof.

endothelial potential of ASCs), whereas hypomethylation seems to have no prediction value on differentiation potential (Boquest *et al*., 2007; Sørensen *et al*., 2009). The present results establish that most endodermal, mesodermal, and ectodermal lineage-specific promoters are hypomethylated, even though differentiation into some of these lineages cannot be achieved by the cell types examined here (Kern *et al*., 2006). Thus, promoter methylation state may constitute a "ground state" program of gene activation potential, with strong methylation being repressive and hypomethylation being potentially permissive (Figure 9B). This model is compatible with a lineage-priming model of MSC differentiation (Boquest *et al*., 2006; Delorme *et al*., 2009).

The core of methylated genes identified in progenitor cells suggests that methylation is established before organogenesis and reflects inaccessibility to developmental programs no longer enabled. These genes are DNA methylated without any of the histone modifications examined here, or are coenriched in the repressive H3K27me3 (Figure 9A). This view is supported by ES cell differentiation studies showing that de novo DNA methylation occurs on pluripotency-associated loci when cells lose pluripotency, whereas subsequent terminal differentiation is accompanied by surprisingly only few methylation changes (Meissner *et al*., 2008; Mohn *et al*., 2008). Similarly, we show here that the majority of hypermethylated promoters in undifferentiated adipogenic or myogenic progenitors retain their methylation state after differentiation (Figure 9C). This indicates that the promoter methylation patterns of differentiated cells are already largely established at the progenitor stage.

A comprehensive methylation analysis recently identified tissue-specific differentially methylated regions located far from promoters or genes and suggested to undergo methylation changes during development (Irizarry *et al*., 2009; Straussman *et al*., 2009). Thus, promoter methylation is unlikely to be the primary determinant of differentiation programming in the soma; it may, however, be involved in, or result from, additional developmental restrictions upon terminal differentiation. Indeed, it is able to distinguish distantly related cell types such as gametes versus somatic cells (Weber *et al*., 2007), or as shown in this study, differentiated adipocytes versus myocytes, or hematopoietic versus mesenchymal progenitors.

What, then, determines MSC differentiation programs? In undifferentiated ES cells, promoters of early differentiation genes are often DNA hypomethylated and cooccupied by transcriptionally permissive H3K4me3 and repressive H3K27me3, creating a temporarily repressive chromatin state (Azuara *et al*., 2006; Bernstein *et al*., 2006; Mikkelsen *et al*., 2007; Fouse *et al*., 2008; Meissner *et al*., 2008; Mohn *et al*., 2008). Differentiation resolves this "bivalency" by removing trimethylation on H3K27 while maintaining H3K4me3 on expressed genes, whereas genes that remain or become repressed retain H3K27me3. In MSCs, these genes are often DNA methylated in the presence or absence of H3K27me3 (Figure 9A). Lineage-specific promoters involved in terminal differentiation are, however, DNA methylated in ES cells (Fouse *et al*., 2008) but are for the most part unmethylated in MSCs (this study). The view of lineage priming by promoter DNA hypomethylation and co-occupancy by H3K4me3 and H3K27me3 can now be extended to tissue-specific progenitors, including HPCs (Cui *et al*., 2009) and adipose-derived MSCs (this study; Figure 9A).

This and previous studies (Weber *et al*., 2007) indicate that promoter DNA methylation poorly correlates with promoter activity. However, although promoters of active genes can also be methylated, promoters of inactive genes seem to be more prone to a spreading of DNA methylation, particularly over the TSS (Figure 5). In addition, relative to the rest of the region examined, the density of methylated CpG is lower at the TSS regardless of promoter activity, in consistency with earlier findings (Weber *et al*., 2007; Lister *et al*., 2009; Straussman *et al*., 2009). Although constitutively unmethylated CpG islands may be protected from methylation by sequence determinants, the mode of recognition of absence of methylation at the TSS remains currently unknown (Straussman *et al*., 2009). It will be interesting to determine whether this is related to chromatin structure and particularly to the existence of unstable nucleosomes around TSSs, notably among expressed genes (Jin and Felsenfeld, 2007; Henikoff, 2008; Zilberman *et al*., 2008; Jin *et al*., 2009).

ACKNOWLEDGMENTS

We thank Dr. Jan Brinchmann (Oslo University Hospital, Oslo, Norway) for generous gift of HPCs and BMMSCs, Dr. Joel Glover (University of Oslo, Oslo, Norway) for neuronal precursors, Dr. Pritinder Kaur (PeterMac Callum Cancer Centre, Melbourne, Australia) for keratinocytes progenitor cells. We thank Kristin Vekterud for expert technical assistance. This work was supported by the Research Council of Norway and a doctoral stipend from the University of Oslo (to B.M.J.).

REFERENCES

Asbreuk, C. H., van Schaick, H. S., Cox, J. J., Smidt, M. P., and Burbach, J. P. (2002). Survey for paired-like homeodomain gene expression in the hypothalamus: restricted expression patterns of Rx, Alx4 and goosecoid. Neuroscience *114*, 883–889.

Azuara, V., *et al*. (2006). Chromatin signatures of pluripotent cell lines. Nat. Cell Biol. *8*, 532–538.

Bernstein, B. E., *et al*. (2006). A bivalent chromatin structure marks key developmental genes in embryonic stem cells. Cell *125*, 315–326.

Boquest, A. C., Noer, A., and Collas, P. (2006). Epigenetic programming of mesenchymal stem cells from human adipose tissue. Stem Cell Rev. *2*, 319–329.

Boquest, A. C., Noer, A., Sorensen, A. L., Vekterud, K., and Collas, P. (2007). CpG methylation profiles of endothelial cell-specific gene promoter regions in adipose tissue stem cells suggest limited differentiation potential toward the endothelial cell lineage. Stem Cells *25*, 852–861.

Boquest, A. C., Shahdadfar, A., Fronsdal, K., Sigurjonsson, O., Tunheim, S. H., Collas, P., and Brinchmann, J. E. (2005). Isolation and transcription profiling of purified uncultured human stromal stem cells: alteration of gene expression after in vitro cell culture. Mol. Biol. Cell *16*, 1131–1141.

Crisan, M., *et al*. (2008). A perivascular origin for mesenchymal stem cells in multiple human organs. Cell Stem Cell *3*, 301–313.

Cui, K., Zang, C., Roh, T. Y., Schones, D. E., Childs, R. W., Peng, W., and Zhao, K. (2009). Chromatin signatures in multipotent human hematopoietic stem cells indicate the fate of bivalent genes during differentiation. Cell Stem Cell *4*, 80–93.

da Silva, M. L., Caplan, A. I., and Nardi, N. B. (2008). In search of the in vivo identity of mesenchymal stem cells. Stem Cells *26*, 2287–2299.

Dahl, J. A., and Collas, P. (2007). Q^2ChIP, a quick and quantitative chromatin immunoprecipitation assay unravels epigenetic dynamics of developmentally regulated genes in human carcinoma cells. Stem Cells *25*, 1037–1046.

Dahl, J. A., Duggal, S., Coulston, N., Millar, D. S., Melki, J., Shahdadfar, A., Brinchmann, J. E., and Collas, P. (2008). Genetic and epigenetic instability of human bone marrow mesenchymal stem cells expanded in autologous serum or fetal bovine serum. Int. J. Dev. Biol. *52*, 1033–1042.

Dahl, J. A., Reiner, A. H., and Collas, P. (2009). Fast genomic ChIP-chip from 1,000 cells. Genome Biol. *10*, R13.

Dahl, J. A., Reiner, A. H., Klungland, A., Wakayama, T., and Collas, P. (2010). Histone H3 lysine 27 methylation asymmetry on developmentally-regulated promoters distinguish the first two lineages in mouse preimplantation embryos. PLoS ONE *5*, e9150.

De Ugarte, D. A., Alfonso, Z., Zuk, P. A., Elbarbary, A., Zhu, M., Ashjian, P., Benhaim, P., Hedrick, M. H., and Fraser, J. K. (2003a). Differential expression of stem cell mobilization-associated molecules on multi-lineage cells from adipose tissue and bone marrow. Immunol. Lett. *89*, 267–270.

De Ugarte, D. A., *et al*. (2003b). Comparison of multi-lineage cells from human adipose tissue and bone marrow. Cells Tissues Organs *174*, 101–109.

Dellavalle, A., *et al*. (2007). Pericytes of human skeletal muscle are myogenic precursors distinct from satellite cells. Nat. Cell Biol. *9*, 255–267.

Delorme, B., Chateauvieux, S., and Charbord, P. (2006). The concept of mesenchymal stem cells. Regen. Med. *1*, 497–509.

Delorme, B., *et al*. (2009). Specific lineage-priming of bone marrow mesenchymal stem cells provides the molecular framework for their plasticity. Stem Cells *27*, 1142–1151.

Donato, R., Miljan, E. A., Hines, S. J., Aouabdi, S., Pollock, K., Patel, S., Edwards, F. A., and Sinden, J. D. (2007). Differential development of neuronal physiological responsiveness in two human neural stem cell lines. BMC Neurosci. *8*, 36.

Falcon, S., and Gentleman, R. (2007). Using GOstats to test gene lists for GO term association. Bioinformatics *23*, 257–258.

Fouse, S. D., Shen, Y., Pellegrini, M., Cole, S., Meissner, A., Van, N. L., Jaenisch, R., and Fan, G. (2008). Promoter CpG methylation contributes to ES cell gene regulation in parallel with Oct4/Nanog, PcG complex, and histone H3 K4/K27 trimethylation. Cell Stem Cell *2*, 160–169.

Henikoff, S. (2008). Nucleosome destabilization in the epigenetic regulation of gene expression. Nat. Rev. Genet. *9*, 15–26.

Irizarry, R. A., *et al*. (2009). The human colon cancer methylome shows similar hypo- and hypermethylation at conserved tissue-specific CpG island shores. Nat. Genet. *41*, 178–186.

Jaenisch, R., and Bird, A. (2003). Epigenetic regulation of gene expression: how the genome integrates intrinsic and environmental signals. Nat. Genet. *33* (suppl), 245–254.

Jin, C., and Felsenfeld, G. (2007). Nucleosome stability mediated by histone variants H3.3 and H2A.Z. Genes Dev. *21*, 1519–1529.

Jin, C., Zang, C., Wei, G., Cui, K., Peng, W., Zhao, K., and Felsenfeld, G. (2009). H3.3/H2A.Z double variant-containing nucleosomes mark 'nucleosome-free regions' of active promoters and other regulatory regions. Nat. Genet. *41*, 941–945.

Johnson, D. S., *et al*. (2008). Systematic evaluation of variability in ChIP-chip experiments using predefined DNA targets. Genome Res. *18*, 393–403.

Kern, S., Eichler, H., Stoeve, J., Kluter, H., and Bieback, K. (2006). Comparative analysis of mesenchymal stem cells from bone marrow, umbilical cord blood or adipose tissue. Stem Cells *24*, 1294–1301.

Kiel, M. J., and Morrison, S. J. (2006). Maintaining hematopoietic stem cells in the vascular niche. Immunity *25*, 862–864.

Kouzarides, T. (2007). Chromatin modifications and their function. Cell *128*, 693–705.

Li, A., and Kaur, P. (2005). FACS enrichment of human keratinocyte stem cells. Methods Mol. Biol. *289*, 87–96.

Lister, R., *et al*. (2009). Human DNA methylomes at base resolution show widespread epigenomic differences. Nature *462*, 315–322.

Meissner, A., *et al*. (2008). Genome-scale DNA methylation maps of pluripotent and differentiated cells. Nature *454*, 766–770.

Mikkelsen, T. S., *et al*. (2007). Genome-wide maps of chromatin state in pluripotent and lineage-committed cells. Nature *448*, 553–560.

Mohn, F., Weber, M., Rebhan, M., Roloff, T. C., Richter, J., Stadler, M. B., Bibel, M., and Schübeler, D. (2008). Lineage-specific polycomb targets and de novo DNA methylation define restriction and potential of neuronal progenitors. Mol. Cell *30*, 755–766.

Noer, A., Lindeman, L. C., and Collas, P. (2009). Histone H3 modifications associated with differentiation and long-term culture of mesenchymal adipose stem cells. Stem Cells Dev. *18*, 725–735.

Noer, A., Sørensen, A. L., Boquest, A. C., and Collas, P. (2006). Stable CpG hypomethylation of adipogenic promoters in freshly isolated, cultured and differentiated mesenchymal stem cells from adipose tissue. Mol. Biol. Cell *17*, 3543–3556.

Norhany, S., Kouzu, Y., Uzawa, K., Hayama, M., Higo, M., Koike, H., Kasamatu, A., and Tanzawa, H. (2006). Overexpression of PAX5 in oral carcinogenesis. Oncol. Rep. *16*, 1003–1008.

O'Geen, H., Nicolet, C. M., Blahnik, K., Green, R., and Farnham, P. J. (2006). Comparison of sample preparation methods for ChIP-chip assays. Biotechniques *41*, 577–580.

Ooi, S. K., and Bestor, T. H. (2008). The colorful history of active DNA demethylation. Cell *133*, 1145–1148.

Pan, G., Tian, S., Nie, J., Yang, C., Ruotti, V., Wei, H., Jonsdottir, G. A., Stewart, R., and Thomson, J. A. (2007). Whole-genome analysis of histone H3 lysine 4 and lysine 27 methylation in human embryonic stem cells. Cell Stem Cell *1*, 299–312.

Peault, B., Rudnicki, M. A., Torrente, Y., Cossu, G., Tremblay, J. P., Partridge, T., Gussoni, E., Kunkel, L. M., and Huard, J. (2007). Stem and progenitor cells in skeletal muscle development, maintenance, and therapy. Mol. Ther. *15*, 867–877.

Pedemonte, E., Benvenuto, F., Casazza, S., Mancardi, G., Oksenberg, J. R., Uccelli, A., and Baranzini, S. E. (2007). The molecular signature of therapeutic mesenchymal stem cells exposes the architecture of the hematopoietic stem cell niche synapse. BMC. Genomics *8*, 65.

Pillai, A., Mansouri, A., Behringer, R., Westphal, H., and Goulding, M. (2007). Lhx1 and Lhx5 maintain the inhibitory-neurotransmitter status of interneurons in the dorsal spinal cord. Development *134*, 357–366.

Shahdadfar, A., Fronsdal, K., Haug, T., Reinholt, F. P., and Brinchmann, J. E. (2005). In vitro expansion of human mesenchymal stem cells: choice of serum is a determinant of cell proliferation, differentiation, gene expression, and transcriptome stability. Stem Cells *23*, 1357–1366.

Sørensen, A. L., and Collas, P. (2009). Immunoprecipitation of methylated DNA. Methods Mol. Biol. *567*, 249–261.

Sørensen, A. L., Timoskainen, S., West, F. D., Vekterud, K., Boquest, A. C., Ährlund-Richter, L., Stice, S. L., and Collas, P. (2009). Lineage-specific promoter DNA methylation patterns segregate adult progenitor cell types. Stem Cells Dev. doi: 10.1089/scd.2009.0309.

Steidl, U., *et al*. (2004). Primary human CD34+ hematopoietic stem and progenitor cells express functionally active receptors of neuromediators. Blood *104*, 81–88.

Straussman, R., Nejman, D., Roberts, D., Steinfeld, I., Blum, B., Benvenisty, N., Simon, I., Yakhini, Z., and Cedar, H. (2009). Developmental programming of CpG island methylation profiles in the human genome. Nat. Struct. Mol. Biol. *16*, 564–571.

Weber, M., Hellmann, I., Stadler, M. B., Ramos, L., Paabo, S., Rebhan, M., and Schubeler, D. (2007). Distribution, silencing potential and evolutionary impact of promoter DNA methylation in the human genome. Nat. Genet. *39*, 457–466.

Zannettino, A. C., Paton, S., Arthur, A., Khor, F., Itescu, S., Gimble, J. M., and Gronthos, S. (2008). Multipotential human adipose-derived stromal stem cells exhibit a perivascular phenotype in vitro and in vivo. J. Cell. Physiol. *214*, 413–421.

Zhao, X. D., *et al*. (2007). Whole-genome mapping of histone H3 Lys4 and 27 trimethylations reveals distinct genomic compartments in human embryonic stem cells. Cell Stem Cell *1*, 286–298.

Zilberman, D., Coleman-Derr, D., Ballinger, T., and Henikoff, S. (2008). Histone H2A.Z and DNA methylation are mutually antagonistic chromatin marks. Nature *456*, 125–129.